Displacement of brain regions in preterm infants with non-synostotic dolichocephaly investigated by MRI

Andrea U.J. Mewes,[a,b,*] Lilla Zöllei,[c,d] Petra S. Hüppi,[e] Heidelise Als,[f] Gloria B. McAnulty,[f] Terrie E. Inder,[g] William M. Wells,[a,c] and Simon K. Warfield[b,c]

[a]Department of Radiology, Brigham and Women's Hospital, Harvard Medical School, Boston, MA, USA
[b]Computational Radiology Laboratory, Department of Radiology, Children's Hospital, Harvard Medical School, Boston, MA, USA
[c]Computer Science and Artificial Intelligence Laboratory, MIT, Cambridge, MA, USA
[d]Athinoula A. Martinos Center, MGH/NMR Center, Charlestown, MA, USA
[e]Child Development Unit, Department of Pediatrics, University Children's Hospital, Geneva, Switzerland
[f]Department of Psychiatry, Children's Hospital, Harvard Medical School, Boston, MA, USA
[g]Department of Pediatrics, Washington University, St. Louis, MO, USA

Regional investigations of newborn MRI are important to understand the appearance and consequences of early brain injury. Previously, regionalization in neonates has been achieved with a Talairach parcellation, using internal landmarks of the brain. Non-synostotic dolichocephaly defines a bi-temporal narrowing of the preterm infant's head caused by pressure on the immature skull. The impact of dolichocephaly on brain shape and regional brain shift, which may compromise the validity of the parcellation scheme, has not yet been investigated. Twenty-four preterm and 20 fulterm infants were scanned at term equivalent. Skull shapes were investigated by cephalometric measurements and population registration. Brain tissue volumes were calculated to rule out brain injury underlying skull shape differences. The position of Talairach landmarks was evaluated. Cortical structures were segmented to determine a positional shift between both groups. The preterm group displayed dolichocephalic head shapes and had similar brain volumes compared to the mesocephalic fulterm group. In preterm infants, Talairach landmarks were consistently positioned relative to each other and to the skull base, but were displaced with regard to the calvarium. The frontal and superior region was enlarged; central and temporal gyri and sulci were shifted comparing preterm and fulterm infants. We found that, in healthy preterm infants, dolichocephaly led to a shift of cortical structures, but did not influence deep brain structures. We concluded that the validity of a Talairach parcellation scheme is compromised and may lead to a miscalculation of regional brain volumes and inconsistent parcel contents when comparing infant populations with divergent head shapes.
© 2007 Elsevier Inc. All rights reserved.

Keywords: Magnetic resonance imaging; Preterm infants; Head shape; Dolichocephaly; Cephalic index; Parcellation; Brain shift

Introduction

Head circumference and skull shape are parameters that are used to examine brain and skull development in infants (Amin et al., 1997; Gutbrod et al., 2000). As the growing brain influences the growth and expansion of the skull, arrested or delayed brain growth leads to decreased head circumference (Hack et al., 1991; Bartholomeusz et al., 2002). In this case, the head circumference represents the size of the skull as an indirect measure of brain volume and growth. Since magnetic resonance imaging (MRI) became widely available, imaging of newborns has been used to assess brain volumes directly by means of tissue segmentation (Huppi et al., 1998). Information about the volume of certain brain tissues is used to draw conclusions about delayed brain development or brain injury (Toft et al., 1995; Inder, 1999 #32; Tolsa et al., 2004; Inder, 2005 #33).

Recently, there has been increasing effort to apply parcellation schemes in connection with tissue segmentation to allow regional investigation of brain tissue volumes in newborns (Peterson et al., 2003; Sowell et al., 2003). It appears that different perinatal factors directly or indirectly affect brain development in a regional manner

---

 * Corresponding author. Department of Radiology, Wolbach 215, The Children's Hospital, 300 Longwood Avenue, Boston, MA 02115, USA. Fax: +1 617 730 0635.
 E-mail address: mewes@bwh.harvard.edu (A.U.J. Mewes).
 Available online on ScienceDirect (www.sciencedirect.com).

(Kesler et al., 2004; Limperopoulos et al., 2005). Thus, a regional investigation of the newborn brain allows such insights. To date, in the investigation of newborns and especially preterm infants, regional investigation has concentrated on the application of a parcellation scheme in which planes set along landmarks defined by Talairach and Tournoux (1988) are used to partition the brain. This scheme relays on the identification of three landmarks, the anterior and posterior commissure and the genu of the corpus callosum (Peterson et al., 2003; Mewes et al., 2006). Imaging of newborns in general suffers from low image resolution, motion artifacts and low contrast intrinsic to the developing brain. In addition, gyral landmarks, which are being used to parcellate the adult brain (Meyer et al., 1999; Fischl et al., 2004; Makris et al., 2006), evolve and change rapidly during cortical development in the newborn period and thus posing additional challenges. This makes it difficult to identify congruent brain regions in newborn subjects by cortical parcellation. In contrast, the structural formation of the corpus callosum (CC) and adjacent commissures is complete by about 20 weeks of gestation, and they appear well defined in their position and shape on newborn MRI. Thus they can be reliably identified in MRI of preterm infants as landmarks for a Talairach parcellation scheme (Rakic and Yakovlev, 1968; Silver et al., 1982; Katz et al., 1983).

After birth the configuration of the neonate's head changes. Besides significant deviation from the norm indicating serious clinical conditions such as premature closure of the skull sutures (Huang et al., 1998) or hydrocephalus, the infants' head in general adjusts to its new environment. External forces compress the skull transmitted from the padding the infant rests on. This procedure affects the head shape of term and preterm infants similarly, but to a different extent (Largo and Duc, 1978). The resulting shape is correlated to the head and sleep position, which lead to either parietal or occipital flattening of the head (Baum and Searls, 1971; Largo and Duc, 1978; Argenta et al., 1996). Certain secondary conditions, which are common in preterm infants, promote the effect of the external compression, such as neurological deficits or immaturity, which reduces the muscle tone to spontaneously change head position, lack of full bone mineralization and prolonged time periods in the same position (Cartlidge and Rutter, 1988; Hemingway and Oliver, 2000; Hummel and Fortado, 2005). As preterm infants are mostly positioned with their heads sideways, often in a fixed position to facilitate respiratory support (Hummel and Fortado, 2005), their heads frequently show a pronounced elongation and temporal narrowing of the head, called non-synostotic dolichocephaly (NSD) (Cartlidge and Rutter, 1988; Hemingway and Oliver, 2000). NSD is correlated to the degree of prematurity. It is more pronounced in the preterm infants born less mature and with low or very low birth weight for gestational age (Largo and Duc, 1978; Elliman et al., 1986). Although studies have investigated preterm infants head shapes and found dolichocephalic head configurations in all study infants (Elliman et al., 1986), NSD is not inevitable in preterm infants and can be avoided with special care. Water pillows (Marsden, 1980; Schwirian et al., 1986), air mattresses (Cartlidge and Rutter, 1988), frequent positional changes and special positioning techniques have been successfully tested (Hummel and Fortado, 2005), but are not part of the standard intensive care. The impact of NSD on the shape of the brain parenchyma and a possible subsequent shift of the brain tissue has not yet been investigated. In the context of a landmark-based parcellation scheme, a displacement of brain structures subsequent to NSD might introduce a systematic error and influence the reliability of the parcellation method.

In this study, we aimed to investigate whether a dolichocephalic skull shape in a group of preterm infants without brain injury led to a displacement of deep or superficial brain structures in comparison to fullterm infants with mesocephalic skulls. We first evaluated whether internal landmarks as defined by Talairach and Tournoux were consistently positioned between the preterm and fullterm study infants (Talairach and Tournoux, 1988). Second, we determined whether specific sulci and gyri were consistently positioned with respect to the deep brain landmarks of the Talairach parcellation scheme.

Methods

Subjects

The scans of forty-four infants born at one of three collaborating medical centers were analyzed in this study. Seven preterm and fourteen fullterm infants were inborn patients at the Royal Women's Hospital in Melbourne, Australia; ten preterm and six fullterm infants were born at the Brigham and Women's Hospital, Boston MA, USA; seven preterm infants were born at the Children's Hospital, Geneva, Switzerland.

Infants enrolled in the study were appropriate for gestational age with head circumference and weight between the 10th and 90th percentile at birth, a five-minute Apgar score ≥7. Preterm infants were born between 28 and 33 weeks (w) gestational age. The gestational age at birth was estimated from the first day of the mother's last menstrual period and the fetus's age in early ultrasound. The post-menstrual age (PMA) of the infants at the time of the scan was computed as the gestational age at birth plus the time elapsed since birth (Engle, 2004). All infants had a normal MRI and cranial ultrasound and required less than 72 h of mechanical ventilation and vasopressor medication. Infants were excluded from the study if they displayed congenital or chromosomal abnormalities, congenital or acquired infections, prenatal brain lesions (e.g. cysts, infarctions) or neonatal seizures. The parents were selected to have no major medical and psychiatric illness, long-term medication treatment (e.g. insulin, antidepressants, anticonvulsants, steroids) and to have no history of substance abuse including tobacco and alcohol. Written informed consent was obtained from all parents prior to enrollment into the study. Permission to scan the infants was granted from the three institutions' Review Boards for Research with Human Subjects.

MRI acquisitions

All MR images were obtained using a 1.5 T MRI system (General Electric Signa, Milwaukee, WI or 1.5 T Marconi Philipps Medical Systems, Andover, MA, USA). Infants were fed 30 min prior to scanning, wrapped in a blanket to avoid arm movement, outfitted with hearing protection, placed on a vacuum pillow and scanned in natural sleep without sedation. Infants were monitored by electrocardiography and pulse oximetry when necessary. Scanning consisted of a high-resolution T1 weighted 3D-Fourier Transform Spoiled Gradient Recalled (SPGR) sequence (0.7×0.7 mm coronal slices, 1.5 mm contiguous slice thickness, 18 cm field of view, matrix 256×256, repetition and echo times of 40 ms and 4 ms, flip angle=20°, scanning time 12 min) and a dual echo

fast spin echo sequence to acquire T2 weighted and proton density weighted images ($0.7 \times 0.7 \times 3$ mm coronal slices, 18 cm field of view, matrix 256×256, 3 mm skip interleave, echo train length = 8, 2 acquisitions: repetition time 4000, echo times 160 ms and 80 ms, 1 NEX, scanning time 6 min). Identical imaging study protocols were used at the three institutions participating in the study to ensure comparability of the scans and to eliminate sources of errors introduced by differences in field strength, scan directions and scan resolution (Patwardhan et al., 2001; Gurleyik and Haacke, 2002). Scanner quality control procedures, including the acquisition of phantom scans, were performed regularly at each site to minimize calibration differences and geometric distortion. In addition, the measurements of the distances between internal structures and the diameters of the skull and the parcellation were tested for statistically significant site dependent differences to identify residual geometric distortion and no such dependency was found.

A pediatric neuro-radiologist reviewed all infants' scans. No infant demonstrated any grade of intraventricular hemorrhage, moderate diffuse or cystic white matter injury or any other focal neuropathology. In addition, a neuro-imaging expert evaluated motion artifacts in each scan and placed the scans in one or two of the following categories: (a) no motion artifacts present; (b) motion artifacts present, but no anatomical ambiguity; (c) motion artifacts and anatomical ambiguity present; (d) the automatic tissue classification, which utilizes the T1 and T2 acquisition simultaneously, showed misclassification due to motion artifacts. The scans of six infants fell into group (c) or (d) and were excluded from further analysis. Another infant had an incomplete scan and was excluded as well. This decreased the initial number of 51 infants to the final 44 subjects, 20 fullterm and 24 preterm infants, whose scans constituted the data considered in this study. At the day of the scan, the preterm infants' PMA was 41.4 ± 1.8 weeks

(mean ± standard deviation) and the fullterm infants' PMA was 41.4 ± 1.1 weeks.

Image processing

Distances, angles and surfaces evaluated in this study were measured using 3D Slicer (Gering et al., 2001). All diameters and distances were measured in millimeter and angles in degree. Sagittal and axial slices were reconstructed from the coronal SPGR image acquisition to ensure accurate alignment and reliable placing of fiducial markers on prominent anatomical landmarks. The identification of cephalometric landmarks (Fig. 1) followed the description given by Swennen et al. (2006). The SPGR image acquisitions were manually rotated and translated to be in alignment with the Talairach coordinate system (Talairach and Tournoux, 1988). Midline alignment followed the inter-hemispheric fissure. The anterior and posterior commissure (AC and PC) were identified simultaneously in the coronal and sagittal view. A line through the most posterior point of the superior edge of the AC (landmark A) and the central point of the inferior edge of the PC (landmarks B) was defined as the AC–PC line (Talairach and Tournoux, 1988). Horizontal alignment was then achieved with regard to the AC–PC line. All landmarks that were identified on a mid-sagittal plane were placed on the first mid-sagittal slice to the right. The same investigator (A.M.) conducted all measurements.

Aim 1: measurement of skull shape

The positions of the landmarks named below are explained in Fig. 1. The occipito-frontal diameter was defined on the mid-sagittal slice as the distance between the glabella and the maximum occipital point of the skull (Fig. 1). The bi-temporal diameter was
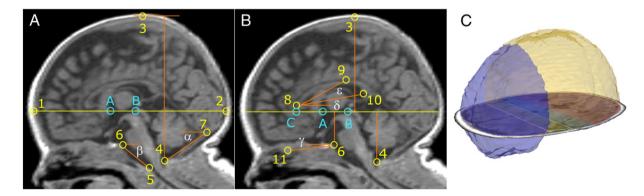

Fig. 1. Landmarks, distances, angles and parcellation results. Image A: landmarks used to investigate the shape of the skull and the parenchyma. Landmark A: most posterior point of the superior edge of the AC; landmark B: central point of the inferior edge of the PC; 1: glabella* (most anterior point of the frontal bone); 2: maximum occipital point (most posterior point of the occipital bone); 3: vertex* (highest point of the cranial vault); 4: opisthion* (mid-sagittal point on the posterior margin of the foramen magnum); 5: basion* (mid-sagittal point on the anterior margin of the foramen magnum); 6: most superior point of the dorsum sellae; 7: superior edge of the protuberance occipitalis. Measurements included the occipito-frontal diameter (1 to 2), the vertical calvarial diameter (3 to 4); α: angle of the posterior cranial fossa; β: the clivus angle. Image B: landmarks used to investigate the position and shape of the Talairach landmarks. Landmark C: most anterior inferior point of the genu of the CC projected on the AC–PC line; 8: most anterior point of the genu of the CC (landmark D); 9: highest most anterior point of the body of the CC; 10: inferior tip of the splenium of the corpus callosum (landmark E); 11: the most inferior point of the anterior cranial fossa projected on the mid-sagittal slice. Measurements made included the length of the CC (C to 10); the diameter of the precentral parcel (8 to A), the central parcel (A to B); the distance AC–PC line (through A and B) to 6 to 4 and to 3; as well as the angle measuring the opening of the posterior CC (δ); the CC angle (ε) and the angle of the anterior cranial fossa (γ). Landmarks A–C (bright blue) as defined by Talairach and Tournoux (Talairach and Tournoux, 1988). Image C shows 3D models of the frontal region (blue) and the superior ICC (yellow), which were significantly enlarged in preterm infants. Also displayed is an axial SPGR slide with the outlined parcellated regions superimposed. * As described in Swennen et al. (2006).

measured in the axial view from the right to the left zygion (the most lateral point of the zygomatic arch). The vertical calvarial diameter was defined on the mid-sagittal slice as the distance from the center point between opisthion and basion to the cranial vertex (Fig. 1). The cephalic index was computed as the ratio of the occipito-frontal and bi-temporal diameter in percent. The shape of the brain parenchyma was investigated measuring the largest occipito-frontal diameter on the mid-sagittal slice and the largest bi-temporal in the axial view.

The landmarks positioned on the calvarium were identified at the inner table of the skull for the following reasons. A chemical shift artifact concerning the representation of the subcutaneous and bone marrow fat in the MRI scans was observed. The display of the bone marrow in the images appeared shifted across the outer table of the skull in the frequency encoding direction of the MRI scan. This artifact in conjunction with the thin skull bone in newborns made it impossible to differentiate between the single layers of the skull. In contrast, the inside border between the fatty tissue with high signal intensity and the inner table of the skull with very low signal intensity was well defined in all three axes of the scan to ensure reliable measurements. Another reason to choose the inner skull table for cephalometric measurements is the high variability of the skull, muscle and skin thickness. Historically, anthropometric measurements have been performed on the outside of the skull to estimate the size of the cranial vault (Lee and Pearson, 1901), although an error was introduced by variable skull thickness between subjects. In infants and children the variability of the skull thickness is especially high due to variations in skull growth, in the development of a continuous dipole and in the onset pneumatization of the frontal skull (Garfin et al., 1986; Wong and Haynes, 1994). Since it has been possible to perform cephalometry on radiographs, computed tomography or MRI, various methods have been developed and validated (Cotton et al., 2005) that use the inner table of the skull with the goal to achieve a measurement of the intra-cranial cavity unbiased by the variability of the skull thickness (Dekaban and Lieberman, 1964; Cronqvist, 1968; Austin and Gooding, 1971).

All angular measurements at the skull base were executed on the mid-sagittal slice. The angle of the posterior cranial fossa (angle α, Fig. 1) was identified as follows: the vertex was defined as the point above the internal occipital protuberance on the skull, the lower line led to the opisthion, the upper line was defined as a parallel of the AC–PC line. The most superior point of the dorsum sellae defined the vertex of the clivus angle (angle β). One line led from the angle's vertex to the basion and a line parallel to the AC–PC line defined the second line. The angle at the foramen magnum was calculated as 180° minus the sum of the posterior fossa angle and the clivus angle. The angulation of the brainstem was measured with the vertex of the angle placed on the pontomedullary sulcus of the brainstem, one line set parallel to the AC–PC line, the second line was placed from the vertex to the anterior border of the brainstem in the center of the foramen magnum.

In addition to the investigation of head shape characteristics based on the identification of landmarks, a population registration method was applied, which utilizes the inter-image data and searches for global shape differences. The group-wise registration algorithm of our choice searches for a 12-parameter global affine transformation associated with each input volume by minimizing over the sum of voxel-wise entropy measures (Miller, 2002; Zöllei, 2006). This fully automatic approach establishes the central tendency of the population without choosing any prior template

or atlas as a reference and thus results in an unbiased representation for further statistical studies. After the alignment, the resulting alignment matrices were investigated for scaling and shearing differences. Translation and rotation differences were removed before the final analysis as these parameters describe differences in the infants' position in the scanner and were not of importance to our investigation. We hypothesized that differences in the alignment matrices identifying differences in the head shapes between our populations will be related to differences along the scaling axes and the size of the shearing parameter.

Aim 2: comparison of brain tissue volumes derived by automatic tissue classification

Volumes of total cerebral parenchyma (CPAR), total intra-cranial cavity (ICC), cerebro-spinal fluid (CSF) and five brain tissues (cortical gray matter (CGM), subcortical gray matter (SGM), unmyelinated (UMWM), myelinated (MWM) white matter and cerebellum (CER)) were assessed to rule out brain injury, which might influence the skull size and shape.

The tissue classification method used in this multi-site study accommodated signal intensity variations between scans. During the segmentation process, the decision whether a voxel belonged to a certain brain tissue class was made relative to all intensity values in the scan and the proportionality of their occurrence. Therefore, although the signal intensity variance in T1 and T2 acquisitions that can occur from inter-scanner variability might have impacted absolute intensity values, such a signal variance did not impact the affiliation of a voxel to a certain tissue class (Warfield et al., 2000). The method has been described elsewhere in detail, validated for newborn MRI (Warfield et al., 2000; Limperopoulos et al., 2005; Mewes et al., 2006) and applied in previous studies (Tolsa et al., 2004; Inder et al., 2005).

Aim 3: determination of position and size of Talairach landmarks

Several diameters and angles were chosen to investigate whether the AC, PC and the CC are consistently positioned in the two groups. It was investigated whether the distances of the AC, PC and CC to one another or the skull was altered reflecting the overall elongation of the brain. The CC shows a special growth pattern during fetal brain development extending from the front to the back while at the same time changing to a curved shape (Hinrichsen, 1990; Hewitt, 1962; Rakic and Yakovlev, 1968). An elongation and narrowing of the brain might have led either to an elongation with a flatter curvature or a wider posterior opening of the CC in the preterm infants compared when to the fullterm infants.

The distance between landmark A and C (the projection of the most anterior inferior point of the CC on the AC–PC line) and the distance between landmark A and B were measured. The length of the CC was determined from the most anterior point of the genu of the CC (landmark D) to the inferior tip of the splenium of the CC (landmark E) (Fig. 1). Also, two angles describing the shape of the CC were evaluated. An angle quantifying the posterior opening of the CC (angle δ) was defined by landmark D as the vertex of the angle, one line leading through landmark E and the second line running parallel to the AC–PC line. Landmark D also marked the vertex of the CC angle (angle ε), landmark E and the highest most anterior point of the CC body defined the lines (Fig. 1).

To investigate whether internal landmarks were displaced with regard to the skull base, the distance between the AC–PC line to the most superior point of the dorsum sellae and the distance to the opisthion were measured. In order to investigate oblique displacement, the angle of the anterior cranial fossa (angle γ) was determined with the vertex being the most superior point of the dorsum sellae, one line parallel to AC–PC line through the vertex, and the second line through the most inferior point of the anterior cranial fossa projected on the mid-sagittal slice.

The distances of the internal landmarks to the calvarium were assessed to investigate whether their relation had changed. Measurements included the distance of the AC–PC line to the cranial vertex and, measured along the AC–PC line, the distance of landmark A to the frontal border of the ICC and the distance of landmark B to the occipital border of the ICC (Fig. 1).

Aim 4: comparison of parcellation results

Five planes oriented along three landmarks (Talairach and Tournoux, 1988) were placed using 3D Slicer to achieve a parcellation of the ICC. A sagittal plane was placed along the inter-hemispherical fissure separating the ICC into a left and a right half. A horizontal plane along the AC–PC line divided the ICC into a superior and inferior part (see also Fig. 3). Finally, three coronal planes through landmark A, B and C partitioned the ICC into four regions. The frontal region included the frontal ICC to landmark C, the precentral region ranged from landmark C to A, the central from landmark A to B and the occipital region included the posterior part of the brain starting from landmark B. Each region consisted of four parcels resulting from the sagittal and horizontal separation: a superior and an inferior parcel on the left and the right hemisphere. Thus, it was possible to investigate the volumes of the total, superior and inferior ICC, sixteen single parcels as well as four regions after adding up the four parcels that belonged to one region. This parcellation scheme has been previously applied and validated for newborn imaging (Peterson et al., 2003; Mewes et al., 2006). Volumes and surfaces of the total, superior and inferior ICC and the four regions were evaluated for significant differences between the pre- and fullterm infants.

Aim 5: investigation of the dispersion of cortical structures across parcels borders

The ten preterm and ten fullterm infants with the smallest and the largest cephalic index, respectively, were chosen to investigate whether specific sulci and gyri were consistently positioned with respect to the deep brain landmarks of the Talairach parcellation scheme. All structures were segmented on the right hemisphere.

The central, precentral and superior frontal sulci were segmented in the axial view. The three structures were identified by the superior–frontal–sulcus–precentral–sulcus sign, the Hook sign, the pars bracket sign, the bifid post-central sulcus sign and the midline sulcus sign (Naidich and Brightbill, 2003). Segmentation started on the most superior axial slice on which the central sulcus could be identified. The sulci were segmented on the slices covering 80% of the parietal lobe measured from the most superior point to the Sylvian fissure. The Sylvian fissure and the superior temporal sulcus were segmented on the coronal slices. The segmentation process started on the most anterior coronal slice, on which the temporal lobe was seen conjoint with the main brain parenchyma. Segmentation continued to the end of the ramus horizontalis of the Sylvian fissure.

The segmentation of the superior temporal gyrus followed the method established by Hirayasu et al. (1998). The inferior frontal and the orbito-frontal sulci were traced using axial and coronal slices following guidelines established and validated by the LONI group (Thompson et al., 1997; Narr et al., 2001). Cuneus, lingula and the calcarine fissure of the occipital lobe were segmented on the four most mid-sagittal slices.

Statistical analyses and validation

All measurements of diameters and angles collected to evaluate the skull shape, tissue volumes, parcellation results and the location of deep brain structures were tested for group differences using analysis of covariance (ANCOVA, probability level, two-tailed: $p < 0.05$) with SPSS (SPSS Inc., Chicago, IL, Version 11.5.1). Model testing was carried out with total ICC and PMA at scan as covariates as well as 2-way interactions between the tested parameter and the covariates. Models with PMA as covariate showed highest significance. The data were tested to ensure that no data assumptions were violated, especially the assumption of the homogeneity of variances and covariate regression coefficients. No evidence for heterogeneity was found. A general linear model implementation of ANCOVA was chosen that uses a Type III method to compute the sum of squares, which is invariant with respect to unequal samples.

A multivariate non-parametric test for two samples of vectors or matrices, called Cramér test, was applied to compare the distribution of manually outlined cortical structures across parcels between the two populations (Franz, 2000; Baringhaus and Franz, 2004). An implementation of the Cramér test in R (Franz, 2006; R Development Core Team, 2006) was used for statistical analysis. For each segmented gyrus or sulcus, the numbers of voxels of a segmented structure present in a parcel were computed. A probability distribution was then constructed for each case, representing the probability of a segmented voxel to belong to a certain parcel. The Cramér test was then applied to compare the probability distributions between preterm and fullterm infants. The confidence level was set to be 0.95; an exponential kernel function (Bahr, 1996) and a permutation Monte-Carlo-Bootstrap method were chosen to estimate the critical value.

The false discovery rate (FDR) by Benjamini and Hochberg (1995) was calculated to control the probability of the family-wise error rate (Hochberg and Tamhane, 1987). For each of the five aims of this project, the number of hypotheses was counted separately before applying the FDR method.

The validity and reliability of the methods that were used to achieve the cephalometric measurements and the manual segmentations of cortical structures have been previously established in adult data. In addition, the intra-observer variability was established on the neonate data used in the current study. For this purpose, the same observer, who performed all other measurements in this study, measured angle ε, angle δ, the length of the CC and the distance from the AC–PC line to the vertex (Fig. 1) five times in five randomly selected subjects. The central sulcus was segmented five times in three different subjects by the same observer. As the position and dispersion of the cortical structures across parcels rather than the volume were of interest in this study, the repeated segmentations of the central sulcus were used to compute the number of segmented voxels that belonged to either the central or the occipital parcel. The ratio of the number of voxels of the central sulcus present in the central to the occipital parcel was then computed for each case and

Table 1
Results of the shape analysis of the skull and parenchyma

Evaluated measurements	Preterm infants	Fullterm infants	*p*-value
DM skull occipito-frontal	122.9±5.6	118.9±4.0	**0.0027**
DM skull bi-temporal	87.7±4.9	93.2±3.2	**<0.0001**
Cephalic index	71.4±2.9	78.4±3.0	**<0.00001**
DM vertical calvarial	95.7±4.3	93.1±5.5	**0.032**
DM CPAR occipito-frontal	114.8±5.5	112.0±4.2	**0.023**
DM CPAR bi-temporal	86.6±4.4	92.8±3.8	**<0.0001**
AN posterior cranial fossa	40.3±5.6	46.0±5.8	**0.002**
AN clivus	46.9±4.2	44.4±5.4	0.093
AN at foramen magnum	92.8±5.8	89.6±7.6	0.127
AN at inferior brainstem	111.7±4.6	120.2±4.2	**<0.0001**

All measurements were analyzed for differences between preterm ($n=24$) and fullterm infants ($n=20$) using ANCOVA. Results are given as mean± standard deviation. *p*-values are considered significant when printed in bold. DM=Diameters (unit: millimeter); AN=angles (unit: degree).

each repetition. The coefficient of variation of the repeated cephalometric measurements and the ratios achieved from the central sulcus segmentations were computed to evaluate the variability of the applied method.

Results

Validation

Repeated measurements of two distances, the CC length and the diameter of the superior ICC, as well as two angles, the angle ε

and angle δ were analyzed for the intra-observer variability. The mean coefficient of variation was 0.99% for the two distances and 3.6% for the two angles. The ratio of the distribution of repeated segmentations of the central sulcus over the central and occipital parcel was analyzed for the intra-observer variability as well. The mean coefficient of variation was 4.1% for the dispersion ratio. With the coefficient of the repeated measurements and segmentations being considerably lower than 10%, the methods used in this study showed good intra-observer reliability.

Measurement of skull shape differences

The occipito-frontal diameter of the skull, the CPAR and the vertical calvarial diameter were significantly larger in preterm infants (Table 1). The bi-temporal diameter of the skull and the CPAR was significantly smaller in preterm infants. Consistent with these findings, the cephalic index was dolichocephalic, under 75, in preterm infants and mesocephalic, above 75, in fullterm infants (Table 1). Visual inspection of the registered preterm scans also showed a smaller bi-temporal diameter of the skull with regard to its length, as well as a rounder and higher shape of the frontal skull than in fullterm infants (Fig. 2). Permutation testing of the alignment matrices revealed a significantly larger scaling factor in the *x* direction in preterm infants ($p=0.0115$) and significantly different shearing parameter in the *xy* ($p=0.0139$) and the *xz* ($p=0.0149$) direction (Fig. 2). The posterior cranial fossa angle and the angulation of the brainstem were significantly smaller in preterm infants (Table 1) indicating a flattening of the posterior fossa simultaneously to the elongation of the skull.
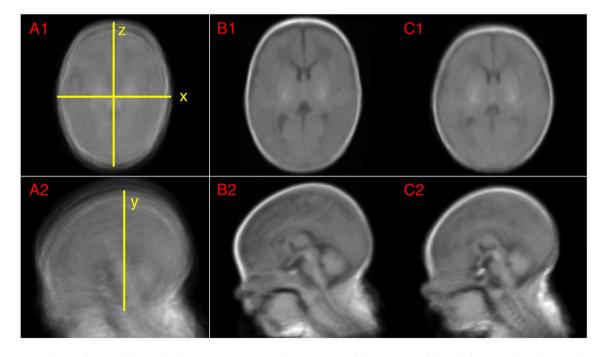

Fig. 2. Mean skull shapes after population registration. Images A1 and A2 show the scans of all preterm and fullterm infants added up after pre-alignment to the Talairach coordinates. The results of the population registration of all preterm scans are shown in image B1 and B2, and the result for congealing all fullterm infants is displayed in image C1 and C2. The upper row displays mid-axial slices; the lower row shows mid-sagittal slices. Note the differences in head shape between B and C: head breadth is increased and head length is decreased in fullterm infants (images B1 and C1). The forehead is flat in fullterm infants (C2) and round in preterm infants (B2). The resulting registration matrices were investigated for scaling and shearing differences in *x*, *y* and *z* direction (yellow marks in A1 and A2).

Table 2
Analysis of the position and the shape of the internal Talairach landmarks

Evaluated measurements	Preterm infants	Fullterm infants	p-value
Internal landmarks to one another			
Length CC	39.1±2.5	38.3±2.4	0.292
Diameter precentral parcel	15.9±1.6	16.9±1.9	0.043
Diameter central parcel	16.3±1.2	16.0±0.9	0.303
Angle AC–PC to posterior CC	42.4±4.4	40.5±3.1	0.096
Angle CC	31.8±6.7	31.4±5.5	0.826
Internal landmarks to skull base			
Distance AC–PC line to dorsum sellae	19.7±1.4	20.1±1.5	0.272
Distance AC–PC line to opisthion	39.1±1.9	40.2±2.0	0.042
Angle anterior cranial fossa	5.5±2.3	5.2±3.2	0.676
Internal landmarks to calvarium			
Distance AC–PC line to cranial vertex	56.5±3.2	53.0±4.3	**0.0008**
Distance AC to frontal border ICC	32.0±2.2	29.1±2.1	**0.0001**
Distance PC to occipital border ICC	54.9±3.8	52.2±3.2	**0.0127**

Diameters, distances, lengths (unit: millimeter) and angles (unit: degree) were analyzed for differences between preterm ($n=24$) and fullterm infants ($n=20$) using ANCOVA. Results are given as mean±standard deviation. p-values are considered significant when printed in bold. CC=corpus callosum; AC=anterior commissure; PC=posterior commissure, ICC= intra-cranial cavity.

Comparison of ICC and brain tissue volumes derived by automatic tissue classification

The volumes of the ICC (preterm: 494.6±59.2 ml; fullterm: 475.8±53.5 ml; $p=0.15$), CPAR (preterm: 434.1±41.0 ml; fullterm: 429.4±41.0 ml; $p=0.63$) and CSF (preterm: 59.7±28.7 ml; fullterm: 45.3±27.8 ml; $p=0.11$) were not significantly different between preterm and fullterm infants. Similar, the total volume of the CGM (preterm: 173.8±28.6 ml; preterm: 163.5±24.7 ml; $p=0.17$), the SGM (preterm: 19.3±5.3 ml; fullterm: 19.2±4.3 ml; $p=0.94$), the UMWM (preterm: 206.8±25.3 ml; fullterm: 210.9± 28.2 ml; $p=0.34$) and the CER (preterm: 26.9±3.8 ml; fullterm: 26.0±3.9 ml; $p=0.47$) were not different between the two groups. Only the volume of the MWM (preterm: 7.3±1.9 ml; fullterm: 9.7±2.7 ml; $p=0.0006$) was significantly decreased in preterm infants. Around 42 weeks PMA, the time point of the scan, myelination is still in an early stage of development; MWM presented only 1.7% of the total CPAR. The locations of myelination were appropriate for the infants' PMA with most of the MWM being in the brainstem, the inferior colliculi and the internal capsule. The volume of the total white matter as the sum of UMWM and MWM was not significantly different between the two groups.

Determination of position and size of Talairach landmarks

It was first investigated whether the position of the deep landmarks with respect to one another was changed and whether the appearance of the CC itself was altered. No significant differences between preterm and fullterm infants were found concerning the length of the CC, the distance from the CC to the

AC, which corresponds to the diameter of the precentral region in the parcellation scheme, and the distance from the AC to the PC, which corresponds to the diameter of central region. Also, the angles describing the shape of the CC were not significantly different between the two groups (Table 2). Second, it was investigated whether the internal landmarks were consistently positioned inside the ICC with regard to the skull base. It was found that the distances measured from the AC–PC line to the dorsum sellae and the opisthion as well as the angle of the anterior cranial fossa did not differ significantly between the two groups (Table 2). Finally, the distances from AC and PC to the calvarium were investigated. It was found that the distances from the AC–PC line to the cranial vertex, from the AC to the frontal border of the ICC, and from the PC to the occipital border of the ICC were significantly larger in the preterm infants (Table 2).

Comparison of parcellation results

The volume of the superior ICC and the volume and surface of the frontal region were significantly larger in the preterm infants (Table 3). Subsequent analysis of the inferior and superior frontal region showed that the increase in volume and surface was confined to the superior frontal region (Table 3). The volume of the superior frontal region was increased by 35% and the surface by 15% in the preterm infants.

Investigation of the dispersion of cortical structures across parcel borders

The dispersion of the cortical structures across parcel borders was investigate to analyze positional differences between preterm and fullterm infants. When comparing the location of segmented

Table 3
Parcellation results: comparison of volumes and surfaces of the parcellated ICC

Parcellated region	Preterm infants	Fullterm infants	p-value
Volumes			
ICC superior	329.0±39.1	305.3±35.5	**0.0084**
ICC inferior	170.2±21.1	172.6±17.9	0.6625
Frontal region	82.9±12.7	68.9±11.6	**0.0002**
Precentral region	80.8±12.1	82.8±10.5	0.5063
Central region	99.7±10.8	101.3±9.6	0.5571
Occipital region	235.9±28.0	225.0±27.4	0.0829
Superior frontal region	55.4±9.1	41.1±7.5	**0.0000**
Inferior frontal region	27.5±4.6	27.8±5.6	0.8235
Surfaces			
ICC total	354.5±29.0	344.6±24.8	0.1198
ICC superior	278.8±22.8	268.6±19.0	0.0364
ICC inferior	237.6±20.8	237.9±15.2	0.9993
Frontal region	119.8±11.6	109.6±12.2	**0.0033**
Precentral region	148.2±13.2	149.7±12.0	0.6797
Central region	170.2±13.3	172.5±13.3	0.5463
Occipital region	227.4±19.3	223.2±18.7	0.3236
Superior frontal region	94.7±9.8	82.3±9.5	**0.0001**
Inferior frontal region	62.4±6.4	61.9±7.1	0.7460

Volumes (unit: milliliter) and surfaces (unit: centimeter squared) were analyzed for differences between preterm ($n=24$) and fullterm infants ($n=20$) using ANCOVA. Results are given as mean±standard deviation. p-values are considered significant when printed in bold. ICC=intra-cranial cavity.

Table 4
Analysis of the overlap of gyri and sulci with the parcellation borders

Segmented structure	Present in parcels	p-value
Orbito-frontal gyrus	FRO+PRE superior+inferior	0.360
Inferior frontal gyrus	FRO+PRE superior+inferior, CEN superior	0.407
Superior frontal sulcus	FRO+PRE+CEN superior	0.644
Precentral sulcus	PRE+CEN superior	**0.006**
Central sulcus	PRE+CEN+OCC superior	0.479
Sylvian fissure	FRO+CEN superior+inferior, OCC superior	**0.012**
Superior temporal gyrus	PRE+CEN+OCC superior+inferior	**0.008**
Calcarine fissure	OCC superior+inferior	0.743
Cuneus	OCC superior+inferior	0.630
Lingula	OCC superior+inferior	0.545

Statistical analysis for the probability of a cortical structure to be present in a certain parcel was conducted using the Cramér Test. The differences in the distribution of a segmented structure between preterm ($n=24$) and fullterm infants ($n=20$) were tested. p-values are considered significant when printed in bold. FRO=frontal parcel; PRE=precentral parcel; CEN=central parcel; OCC=occipital parcel.

gyri with respect to the parcellation borders, cortical structures segmented in a certain lobe were spread about up to six different parcels (Table 4). For example, the segmented Sylvian fissure was found in the superior and inferior precentral and central parcels as well as in the superior occipital parcel (Fig. 3).

Of all cortical structures segmented in the current study, the Cramér test results showed significantly different distributions across parcels between the two groups for the Sylvian fissure, the superior temporal gyrus and the precentral sulcus (Table 4, Fig. 3).

Discussion

During infancy, the growing skull and the developing brain interact with each other and eventually achieve the adult shape and size of the head and brain. Brain injury may interfere with skull growth (Hack et al., 1991) and skull growth that diverges from its normal trajectory may lead to a dysmorphology of the brain (Aldridge et al., 2002). The preterm infants in this study demonstrated an occipito-frontal and inferior–superior elongation and a temporal narrowing of the skull together with a flattening of the occipital skull base. These preterm infants were healthy with minimal perinatal or postnatal risk factors and no evidence of brain injury or craniosynostosis. In addition, there was no loss of brain tissue identified, which could have accounted for shape differences. Therefore, the head deformation was best defined as non-synostotic dolichocephaly, a form of positional molding that appears to results from external pressure on the immature skull bone after premature birth.

As a result of such skull deformation, the AC, PC and the CC appeared to be placed at greater distance from the anterior,
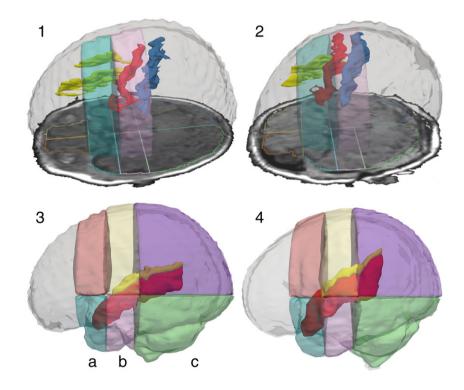

Fig. 3. 3D models of segmented gyri and sulci in relation to parcel borders. The upper row shows 3D models of the superior frontal sulcus (yellow), the precentral sulcus (red) and the central sulcus (blue) inside a model of the ICC. The sulci segmentations are overlaid by transparent models of the superior precentral parcel (bright blue) and the superior central parcel (rose). An axial SPGR slide with an outline of the parcellation is also to be seen. Image 1 displays a preterm infant' segmentation, image 2 displays a fullterm case. Two representative cases were chosen to visualize how the precentral sulcus is almost entirely shifted into the central region in preterm infants. The lower row shows 3D models of the superior temporal gyrus (red) and the Sylvian fissure (yellow) overlaid by 3D models of the superior and inferior precentral (a), central (b) and occipital parcels (c). Image 3 displays a preterm case, image 4 a fullterm case. Note how in the preterm infant the superior temporal gyrus and the Sylvian fissure are shifted downwards and show a flat orientation with regard to the parcellation in comparison to the fullterm infant.

superior and posterior calvarium. It was hypothesized that the elongation of the skull would affect the internal commissures, and therefore an increase of the AC–PC distance was expected that would have also affected the length and curvature of the CC, given that there is an interaction between position and shape of these structures (Prakash and Nowinski, 2006). Instead, it was found that the positions of the AC, PC and CC relative to each other were in fact consistent as was their position in relation to the skull base. There are several possible explanations why the AC, PC and CC may not have been affected by the skull change in the current study. First, it has to be considered that these structures may be stabilized in their position due to their close vicinity to the brainstem, the visual tract and the sella turcica, which are anchored to the skull base. Second, the telencephalon may shelter the deep brain structures from the external pressure on the skull. Third, the shape of the commissures, which appear early in brain development, is already well defined by the time of preterm birth (Hewitt, 1962; Rakic and Yakovlev, 1968; Katz et al., 1983). In contrast, the cortex, which still undergoes rapid and profound shape and volume changes after premature birth, especially with regard to cortical folding and growth of axonal connectivity, might be more prone to deformation due to external influences such as pressure.

The study's results indicated a shift of cortical structures with respect to the position of the commissures in preterm infants in comparison to fullterm infants studied at the same post-menstrual age. This suggests that the external pressure on the skull does not affect the entire brain and that only parts of the brain closely related to the skull change their shape and position. A similar effect has been found in the case of infants with cranial synostosis, where depending on the extent of the involved suture, brain dysmorphology was unilateral, but in contrast to the results from the current study, also involved displacement of the deep lying brain structures (Aldridge et al., 2005). The data presented in the current study suggest that the impact of an external force influencing the brain morphology is different from the effect of the endogenous cause for cranial synostosis, which from early on continuously influences the skull–brain interaction thus yielding the typical cranial synostotic phenotype (Aldridge et al., 2005; Richtsmeier et al., 2006). The mode of brain deformation in dolichocephaly, in contrast, appears more similar to the tissue displacement described in brain tumors, where mechanical pressure affects the brain regions adjacent to the tumor (Parker and Ongley, 1981; Gordon et al., 2003; Clatz et al., 2005).

When a parcellation scheme is used to investigate regional brain appearance in preterm infants, an over- or underestimation of parcel size due to a systematic error might erroneously indicate decreased tissue volumes, possibly interpreted as brain injury or obscure decreased tissue volumes mimicking normal brain development. After applying a Talairach parcellation scheme to all scans, it was found that the frontal and the superior region were enlarged in the preterm infants. These results must be interpreted in the context of the findings that the total CPAR and ICC were not increased in the preterm infants and that the landmarks used for the parcellation were found to be displaced only in relation to the skull, but not with regard to each other. As a result of the dolichocephalic shape changes, the diameter of the frontal region and the superior ICC was increased in preterm infants as well, while the diameters of the precentral and central region, closely related to the position of the AC and PC, were not different between the groups. Thus, it must be concluded that the enlargement of the frontal and the

superior ICC is an effect of the head shape differences and not a sign of brain developmental differences.

It might be proposed that although the preterm skull is shaped differently, the borders of the parcellation might be shifted in proportion to the skull elongation and narrowing, so that the regional anatomical borders move as well, such that the parcels might still contain comparable anatomical regions. In contrast, a shift of cortical structures was identified that led to inconsistent parcel contents. The results as discussed above indicate that the reliability of a Talairach parcellation scheme, applied with the goal to compare the similarity of brain regions between infant populations, is compromised if the populations under investigation display significantly different head shapes. In recent years, the "Back to Sleep" guidelines of the American Academy of Pediatrics for the prevention of Sudden Infant Death Syndrome (SIDS) have been implemented extensively (American Academy of Pediatrics, 2005; Moon et al., 2004). While successful in decreasing SIDS, an increasing percentage of plagiocephaly and flattened skulls have been reported as a result of the supine sleep position encouraged by this program (Argenta et al., 1996; Hutchison et al., 2003, 2004; Hummel and Fortado, 2005). These specific skull alterations and their possible influence on parcellation techniques must be considered in future attempts to analyze regional brain volumes in preterm and fullterm infants.

Although a Talairach parcellation scheme as the one used in this study yields reliable results if the populations under investigation have comparable head shapes, it is ultimately desirable to apply parcellation techniques that yield anatomically consistent regions despite morphological differences in skull and brain shapes. Such a parcellation scheme might for example consider either white matter compartments (Meyer et al., 1999) or cortical landmarks (Ballmaier et al., 2004; Fischl et al., 2004). In an automatic approach this might only be feasible if different age-dependent atlases were provided, considering the fundamental changes in the gyral patterns in preterm infants from 30 weeks PMA to 3 years of age. In this context, one must carefully evaluate which gyral landmarks are established early enough in cortical development to allow their reliable identification throughout different stages of gyrification. For example, the medium and inferior temporal sulci appear around 34 weeks PMA (Abe et al., 2003) and are therefore not defined at an age where MR scans of preterm infants may be analyzed. Recent approaches have investigated the feasibility of DTI parcellation in adults (Klein et al., 2007). This approach might be considered for preterm imaging as well since it yields a parcellation scheme that defines regions by their functional dependency and is therefore independent of cortical landmarks.

The segmented regions and landmarks selected in the current study, uniquely identified the internal and cortical anatomical structures, whose position and shape have been investigated. They are developmentally stable and appear early during brain growth and could reliably be identified in each subject. In addition, the internal landmarks were also critically related to the parcellation method discussed here. Nevertheless, in the current study only a limited number of cortical and subcortical structures were investigated. It is thus not possible to conclude whether the skull deformation affected other parts of the brain, and if so, how those parts were related to the site of the skull deformation. Different methods, for example, a morphometric approach may be considered for future investigations of shape and position of the entire cortex and subcortical structures. Morphometric methods differ from interactive landmark selection by the identification of characteristic correspondence based on all of the imaging data and require a

registration of all data into a common space. Recently deformation-based morphometry has been used to investigate shape differences (Ashburner et al., 1998; Gaser et al., 1999) and has been applied successfully to investigate volume differences in preterm infants (Boardman et al., 2006) by analyzing local differences in the resulting deformation fields after image alignment. Such a method may be deployed in future projects as an exploratory and non-subjective approach for the investigation of local shape and positional variations of the neonate brain. A careful evaluation of adequate filter and registration parameter settings as well as an evaluation of statistical analyses sufficient to establish statistical significance is critical in such an approach.

It would also be valuable to investigate differences in the sulcal or gyral patterns and complexities besides positional displacements. Asymmetry of the brain has been measured by computing sulcal complexity, sulcus or gyral length as well as number and variability of spatial coordinates in order to investigate gender effects, hemisphere asymmetries and pathogenesis of schizophrenia (Juch et al., 2005; Blanton et al., 2001; Narr et al., 2001). For these observations, genetic determination of sulcal development, neuronal plasticity, myelination and synaptic remodeling have been discussed as possible underlying mechanisms and explanations without taking into account the influences of possible extraneous factors on the morphology of the brain.

In this study, the influence of non-synostotic dolichocephaly on the morphology of subcortical and cortical brain structures was investigated in a group of preterm infants appropriate for gestational age and without brain injury. The results indicate that a shape change of the brain parenchyma affects the superficial areas in close relationship to the skull causing a displacement of cortical structures. A landmark-based parcellation approach showed inconsistent anatomical parcel contents due to the combination of cortical shifting in the presence of unaltered morphology of subcortical brain structures. It is proposed that external pressure on the immature skull leads to a mechanically influenced change in cortical morphology that needs to be considered in regional analyses of the developing brain.

References

Abe, S., Takagi, K., Yamamoto, T., Okuhata, Y., Kato, T., 2003. Assessment of cortical gyrus and sulcus formation using MR images in normal fetuses. Prenat. Diagn. 23, 225–231.

Aldridge, K., Marsh, J.L., Govier, D., Richtsmeier, J.T., 2002. Central nervous system phenotypes in craniosynostosis. J. Anat. 201, 31–39.

Aldridge, K., Kane, A.A., Marsh, J.L., Panchal, J., Boyadjiev, S.A., Yan, P., Govier, D., Ahmad, W., Richtsmeier, J.T., 2005. Brain morphology in nonsyndromic unicoronal craniosynostosis. Anat. Rec., A Discov. Mol. Cell. Evol. Biol. 285, 690–698.

American Academy of Pediatrics, 2005. The changing concept of sudden infant death syndrome: diagnostic coding shifts, controversies regarding the sleeping environment, and new variables to consider in reducing risk. Pediatrics 116, 1245–1255.

Amin, H., Singhal, N., Sauve, R.S., 1997. Impact of intrauterine growth restriction on neurodevelopmental and growth outcomes in very low birthweight infants. Acta Paediatr. 86, 306–314.

Argenta, L.C., David, L.R., Wilson, J.A., Bell, W.O., 1996. An increase in infant cranial deformity with supine sleeping position. J. Craniofac. Surg. 7, 5–11.

Ashburner, J., Hutton, C., Frackowiak, R., Johnsrude, I., Price, C., Friston, K., 1998. Identifying global anatomical differences: deformation-based morphometry. Hum. Brain Mapp. 6, 348–357.

Austin, J.H., Gooding, C.A., 1971. Roentgenographic measurement of skull size in children. Radiology 99, 641–646.

Bahr, R., 1996. Ein neuer Test für das mehrdimensionale Zwei-Stichproben-Problem bei allgemeiner Alternative. PhD thesis. University of Hannover, Hannover, Germany.

Ballmaier, M., Toga, A.W., Blanton, R.E., Sowell, E.R., Lavretsky, H., Peterson, J., Pham, D., Kumar, A., 2004. Anterior cingulate, gyrus rectus, and orbitofrontal abnormalities in elderly depressed patients: an MRI-based parcellation of the prefrontal cortex. Am. J. Psychiatry 161, 99–108.

Baringhaus, L., Franz, C., 2004. On a new multivariate two-sample test. J. Multivar. Anal. 88, 190–206.

Bartholomeusz, H.H., Courchesne, E., Karns, C.M., 2002. Relationship between head circumference and brain volume in healthy normal toddlers, children, and adults. Neuropediatrics 33, 239–241.

Baum, J.D., Searls, D., 1971. Head shape and size of pre-term low-birthweight infants. Dev. Med. Child Neurol. 13, 576–581.

Benjamini, Y., Hochberg, Y., 1995. Controlling the false discovery rate: a practical and powerful approach to multiple testing. J. R. Stat. Soc., Ser. B 57, 289–300.

Blanton, R.E., Levitt, J.G., Thompson, P.M., Narr, K.L., Capetillo-Cunliffe, L., Nobel, A., Singerman, J.D., McCracken, J.T., Toga, A.W., 2001. Mapping cortical asymmetry and complexity patterns in normal children. Psychiatry Res. 107, 29–43.

Boardman, J.P., Counsell, S.J., Rueckert, D., Kapellou, O., Bhatia, K.K., Aljabar, P., Hajnal, J., Allsop, J.M., Rutherford, M.A., Edwards, A.D., 2006. Abnormal deep grey matter development following preterm birth detected using deformation-based morphometry. NeuroImage 32, 70–78.

Cartlidge, P.H., Rutter, N., 1988. Reduction of head flattening in preterm infants. Arch. Dis. Child. 63, 755–757.

Clatz, O., Sermesant, M., Bondiau, P.Y., Delingette, H., Warfield, S.K., Malandain, G., Ayache, N., 2005. Realistic simulation of the 3-D growth of brain tumors in MR images coupling diffusion with biomechanical deformation. IEEE Trans. Med. Imag. 24, 1334–1346.

Cotton, F., Rozzi, F.R., Vallee, B., Pachai, C., Hermier, M., Guihard-Costa, A.M., Froment, J.C., 2005. Cranial sutures and craniometric points detected on MRI. Surg. Radiol. Anat. 27, 64–70.

Cronqvist, S., 1968. Roentgenologic evaluation of cranial size in children. A new index. Acta Radiol.: Diagn. (Stockh.) 7, 97–111.

Dekaban, A., Lieberman, J.E., 1964. Calculation of cranial capacity from linear dimensions. Anat. Rec. 150, 215–219.

Elliman, A.M., Bryan, E.M., Elliman, A.D., Starte, D., 1986. Narrow heads of preterm infants—Do they matter? Dev. Med. Child Neurol. 28, 745–748.

Engle, W.A., 2004. Age terminology during the perinatal period. Pediatrics 114, 1362–1364.

Fischl, B., van der Kouwe, A., Destrieux, C., Halgren, E., Segonne, F., Salat, D.H., Busa, E., Seidman, L.J., Goldstein, J., Kennedy, D., Caviness, V., Makris, N., Rosen, B., Dale, A.M., 2004. Automatically parcellating the human cerebral cortex. Cereb. Cortex 14, 11–22.

Franz, C., 2000. Ein statistischer Test für das mehrdimensionale Zweistich-proben-Problem. In: Institut für Mathematische Stochastik. Diploma thesis. University Hannover, Hannover, Germany.

Franz, C., 2006. The cramer Package, 0.8-1 edn. R Project, Free Software Foundation's GNU Project.

Garfin, S.R., Roux, R., Botte, M.J., Centeno, R., Woo, S.L., 1986. Skull osteology as it affects halo pin placement in children. J. Pediatr. Orthop. 6, 434–436.

Gaser, C., Volz, H.P., Kiebel, S., Riehemann, S., Sauer, H., 1999. Detecting structural changes in whole brain based on nonlinear deformations—Application to schizophrenia research. NeuroImage 10, 107–113.

Gering, D.T., Nabavi, A., Kikinis, R., Hata, N., O'Donnell, L.J., Grimson, W.E., Jolesz, F.A., Black, P.M., Wells 3rd, W.M., 2001. An integrated visualization system for surgical planning and guidance using image fusion and an open MR. J. Magn. Reson. Imaging 13, 967–975.

Gordon, V.D., Valentine, M.T., Gardel, M.L., Andor-Ardo, D., Dennison, S., Bogdanov, A.A., Weitz, D.A., Deisboeck, T.S., 2003. Measuring the mechanical stress induced by an expanding multicellular tumor system: a case study. Exp. Cell Res. 289, 58–66.

Gurleyik, K., Haacke, E.M., 2002. Quantification of errors in volume measurements of the caudate nucleus using magnetic resonance imaging. J. Magn. Reson. Imaging 15, 353–363.

Gutbrod, T., Wolke, D., Soehne, B., Ohrt, B., Riegel, K., 2000. Effects of gestation and birth weight on the growth and development of very low birthweight small for gestational age infants: a matched group comparison. Arch. Dis. Child., Fetal Neonatal Ed. 82, F208–F214.

Hack, M., Breslau, N., Weissman, B., Aram, D., Klein, N., Borawski, E., 1991. Effect of very low birth weight and subnormal head size on cognitive abilities at school age. N. Engl. J. Med. 325, 231–237.

Hemingway, M., Oliver, S., 2000. Bilateral head flattening in hospitalized premature infants. Online J. Knowl. Synth. Nurs. 7, 3.

Hewitt, W., 1962. The development of the human corpus callosum. J. Anat. 96, 355–358.

Hinrichsen, K.V., 1990. Humanembryologie. Lehrbuch und Atlas der vorgeburtlichen Entwicklung des Menschen. Springer, Berlin.

Hirayasu, Y., Shenton, M.E., Salisbury, D.F., Dickey, C.C., Fischer, I.A., Mazzoni, P., Kisler, T., Arakaki, H., Kwon, J.S., Anderson, J.E., Yurgelun-Todd, D., Tohen, M., McCarley, R.W., 1998. Lower left temporal lobe MRI volumes in patients with first-episode schizophrenia compared with psychotic patients with first-episode affective disorder and normal subjects. Am. J. Psychiatry 155, 1384–1391.

Hochberg, Y., Tamhane, A., 1987. Multiple Comparison Procedures. Wiley, New York.

Huang, M.H., Mouradian, W.E., Cohen, S.R., Gruss, J.S., 1998. The differential diagnosis of abnormal head shapes: separating craniosynostosis from positional deformities and normal variants. Cleft Palate-Craniofac. J. 35, 204–211.

Hummel, P., Fortado, D., 2005. Impacting infant head shapes. Adv. Neonatal Care 5, 329–340.

Huppi, P.S., Warfield, S., Kikinis, R., Barnes, P.D., Zientara, G.P., Jolesz, F.A., Tsuji, M.K., Volpe, J.J., 1998. Quantitative magnetic resonance imaging of brain development in premature and mature newborns. Ann. Neurol. 43, 224–235.

Hutchison, B.L., Thompson, J.M., Mitchell, E.A., 2003. Determinants of nonsynostotic plagiocephaly: a case–control study. Pediatrics 112, e316.

Hutchison, B.L., Hutchison, L.A., Thompson, J.M., Mitchell, E.A., 2004. Plagiocephaly and brachycephaly in the first two years of life: a prospective cohort study. Pediatrics 114, 970–980.

Inder, T.E., Warfield, S.K., Wang, H., Huppi, P.S., Volpe, J.J., 2005. Abnormal cerebral structure is present at term in premature infants. Pediatrics 115, 286–294.

Juch, H., Zimine, I., Seghier, M.L., Lazeyras, F., Fasel, J.H., 2005. Anatomical variability of the lateral frontal lobe surface: implication for intersubject variability in language neuroimaging. NeuroImage 24, 504–514.

Katz, M.J., Lasek, R.J., Silver, J., 1983. Ontophyletics of the nervous system: development of the corpus callosum and evolution of axon tracts. Proc. Natl. Acad. Sci. U. S. A. 80, 5936–5940.

Kesler, S.R., Ment, L.R., Vohr, B., Pajot, S.K., Schneider, K.C., Katz, K.H., Ebbitt, T.B., Duncan, C.C., Makuch, R.W., Reiss, A.L., 2004.

Volumetric analysis of regional cerebral development in preterm children. Pediatr. Neurol. 31, 318–325.

Klein, J.C., Behrens, T.E., Robson, M.D., Mackay, C.E., Higham, D.J., Johansen-Berg, H., 2007. Connectivity-based parcellation of human cortex using diffusion MRI: establishing reproducibility, validity and observer independence in BA 44/45 and SMA/pre-SMA. NeuroImage 34, 204–211.

Largo, R.H., Duc, G., 1978. Head growth and changes in head configuration in healthy preterm and term infants during the first sex months of life. Helv. Paediatr. Acta 32, 431–442.

Lee, A., Pearson, K., 1901. Data for the problem of evolution in man—a first study of the correlation of the human skull. Philos. Trans. R. Soc. 196, 225–264.

Limperopoulos, C., Soul, J.S., Gauvreau, K., Huppi, P.S., Warfield, S.K., Bassan, H., Robertson, R.L., Volpe, J.J., du Plessis, A.J., 2005. Late gestation cerebellar growth is rapid and impeded by premature birth. Pediatrics 115, 688–695.

Makris, N., Kaiser, J., Haselgrove, C., Seidman, L.J., Biederman, J., Boriel, D., Valera, E.M., Papadimitriou, G.M., Fischl, B., Caviness Jr., V.S., Kennedy, D.N., 2006. Human cerebral cortex: a system for the integration of volume- and surface-based representations. NeuroImage 33, 139–153.

Marsden, D.J., 1980. Reduction of head flattening in preterm infants. Dev. Med. Child Neurol. 22, 507–509.

Mewes, A.U., Huppi, P.S., Als, H., Rybicki, F.J., Inder, T.E., McAnulty, G.B., Mulkern, R.V., Robertson, R.L., Rivkin, M.J., Warfield, S.K., 2006. Regional brain development in serial magnetic resonance imaging of low-risk preterm infants. Pediatrics 118, 23–33.

Meyer, J.W., Makris, N., Bates, J.F., Caviness, V.S., Kennedy, D.N., 1999. MRI-based topographic parcellation of human cerebral white matter. NeuroImage 9, 1–17.

Miller, E.G., 2002. Learning from one example in machine vision by sharing probability densities. In: Department of Electrical Engineering and Computer Science. PhD thesis, Massachusetts Institute of Technology, Cambridge.

Moon, R.Y., Oden, R.P., Grady, K.C., 2004. Back to sleep: an educational intervention with women, infants, and children program clients. Pediatrics 113, 542–547.

Naidich, T.P., Brightbill, T.C., 2003. Vascular territories and watersheds: a zonal frequency analysis of the gyral and sulcal extent of cerebral infarcts. Part I: the anatomic template. Neuroradiology 45, 536–540.

Narr, K., Thompson, P., Sharma, T., Moussai, J., Zoumalan, C., Rayman, J., Toga, A., 2001. Three-dimensional mapping of gyral shape and cortical surface asymmetries in schizophrenia: gender effects. Am. J. Psychiatry 158, 244–255.

Parker Jr., J.C., Ongley, J.P., 1981. A neuropathologic approach to human disease: the intracranial mass effect. Am. J. Forensic Med. Pathol. 2, 11–17.

Patwardhan, A.J., Eliez, S., Warsofsky, I.S., Glover, G.H., White, C.D., Giedd, J.N., Peterson, B.S., Rojas, D.C., Reiss, A.L., 2001. Effects of image orientation on the comparability of pediatric brain volumes using three-dimensional MR data. J. Comput. Assist. Tomogr. 25, 452–457.

Peterson, B.S., Anderson, A.W., Ehrenkranz, R., Staib, L.H., Tageldin, M., Colson, E., Gore, J.C., Duncan, C.C., Makuch, R., Ment, L.R., 2003. Regional brain volumes and their later neurodevelopmental correlates in term and preterm infants. Pediatrics 111, 939–948.

Prakash, K.N., Nowinski, W.L., 2006. Morphologic relationship among the corpus callosum, fornix, anterior commissure, and posterior commissure MRI-based variability study. Acad. Radiol. 13, 24–35.

R Development Core Team, 2006. R: A Language and Environment for Statistical Computing, 2.4.0 edn. R Foundation for Statistical Computing, Vienna, Austria.

Rakic, P., Yakovlev, P.I., 1968. Development of the corpus callosum and cavum septi in man. J. Comp. Neurol. 132, 45–72.

Richtsmeier, J.T., Aldridge, K., DeLeon, V.B., Panchal, J., Kane, A.A., Marsh, J.L., Yan, P., ColeI 3rd, T.M., 2006. Phenotypic integration of neurocranium and brain. J. Exp. Zool., B Mol. Dev. Evol. 306, 360–378.

Schwirian, P.M., Eesley, T, Cuellar, L., 1986. Use of water pillows in

reducing head shape distortion in preterm infants. Res. Nurs. Health 9, 203–207.

Silver, J., Lorenz, S.E., Wahlsten, D., Coughlin, J., 1982. Axonal guidance during development of the great cerebral commissures: descriptive and experimental studies, in vivo, on the role of preformed glial pathways. J. Comp. Neurol. 210, 10–29.

Sowell, E.R., Thompson, P.M., Welcome, S.E., Henkenius, A.L., Toga, A.W., Peterson, B.S., 2003. Cortical abnormalities in children and adolescents with attention-deficit hyperactivity disorder. Lancet 362, 1699–1707.

Swennen, G.R.J., Schutyser, F., Hausamen, J.-E., 2006. Three-Dimensional Cephalometry: A Color Atlas and Manual. Springer, Berlin.

Talairach, J., Tournoux, P., 1988. Co-Planar Stereotaxic Atlas of the Human Brain. Thieme Medical Publishers, New York.

Thompson, P.M., MacDonald, D., Mega, M.S., Holmes, C.J., Evans, A.C., Toga, A.W., 1997. Detection and mapping of abnormal brain structure with a probabilistic atlas of cortical surfaces. J. Comput. Assist. Tomogr. 21, 567–581.

Toft, P.B., Leth, H., Ring, P.B., Peitersen, B., Lou, H.C., Henriksen, O., 1995. Volumetric analysis of the normal infant brain and in intrauterine growth retardation. Early Hum. Dev. 43, 15–29.

Tolsa, C.B., Zimine, S., Warfield, S.K., Freschi, M., Sancho Rossignol, A., Lazeyras, F., Hanquinet, S., Pfizenmaier, M., Huppi, P.S., 2004. Early alteration of structural and functional brain development in premature infants born with intrauterine growth restriction. Pediatr. Res. 56, 132–138.

Warfield, S.K., Kaus, M., Jolesz, F.A., Kikinis, R., 2000. Adaptive, template moderated, spatially varying statistical classification. Med. Image Anal. 4, 43–55.

Wong, W.B., Haynes, R.J., 1994. Osteology of the pediatric skull. Considerations of halo pin placement. Spine 19, 1451–1454.

Zöllei, L., 2006. A unified information theoretic framework for pair- and group-wise registration of medical images. In: Department of Electrical Engineering and Computer Science. PhD thesis, Massachusetts Institute of Technology, Cambridge.